

# Precision Lead Tungstate Crystal Calorimeter for CMS at LHC

Ren-Yuan Zhu, *Senior Member, IEEE*

**Abstract**—A precision lead tungstate crystal calorimeter is being constructed by the CMS collaboration as a powerful tool to probe electroweak symmetry breaking and new physics in the LHC era. The status of calorimeter construction is reported. A crucial issue of maintaining crystal calorimetry precision in the expected radiation environment is elaborated.

**Index Terms**—Calorimeter, crystal, lead tungstate, monitoring, radiation damage, scintillator.

## I. INTRODUCTION

THE main physics motivation for building the Compact Muon Solenoid (CMS) experiment at the Large Hadron Collider (LHC) is to investigate the mechanism responsible for electroweak symmetry breaking. Other important physics motivations of CMS are to search for supersymmetric particles, to study the properties of the top and the bottom quarks, to search for new forces in the form of massive bosons similar to the W and Z and for compactness of quarks and leptons. Fig. 1 shows a simulation result for a low-mass Higgs search through  $\gamma\gamma$  decay channel measured with a precision electromagnetic calorimeter (ECAL) at LHC [1]. The Higgs discovery potential in this decay channel is directly related to the reconstructed mass width or the ECAL energy resolution.

To exploit the full range of TeV-scale physics at LHC the CMS detector is designed with emphasis on clean identification and precision measurements of electrons, muons, and photons. Combined with good jet and missing energy measurements, the detector has excellent physics potential. The design goal of the CMS detector is to measure electrons, photons and muons with an energy resolution of better than 1% over a large momentum range. The principal detector features include a high resolution and redundant muon system, a lead tungstate ( $\text{PbWO}_4$  or PWO) crystal ECAL and a precision all-silicon tracker. The overall dimensions of the detector are: a length of 21.6 m, a diameter of 15 m and a total weight of 12 500 tons. The hadron calorimeter (HCAL) and the ECAL are located in a large, 13 m long, 6 m diameter, high-field (4T) superconducting solenoid.

## II. PWO CRYSTAL ECAL

The CMS PWO crystal ECAL consists of 76 000 crystals, with a 23 cm ( $25.8 X_0$ ) length, a  $2.2 \times 2.2 \text{ cm}^2$  front face and

a 1.1-kg weight, for a total crystal volume of  $10.8 \text{ m}^3$  and a weight of 90.3 t. It is divided to 36 supermodules (SM) with 1700 channels each in the barrel and 4 Dee's with 3500 channels each in the endcaps. A three-dimensional (3-D) cut-away view of the CMS PWO ECAL is shown in Fig. 2 [1]. Each crystal is read out by two  $0.25 \text{ cm}^2$  Si avalanche photodiodes (APD) in the barrel, and by a low-gain vacuum phototube (VPT) in the endcaps. Each crystal is also coupled to one monitoring fiber for *in situ* monitoring. All readout electronics is designed by using ASICs of  $0.25 \mu\text{m}$  CMOS technology.

The designed energy resolution ( $\Delta E/E$ ) is  $2.5\%/\sqrt{E} \oplus 0.55\% \oplus 0.2/E$  for the barrel and  $5.7\%/\sqrt{E} \oplus 0.55\% \oplus 0.25/E$  for the endcaps, where  $\oplus$  stands for addition in quadrature and E is in GeV. Test beams at CERN have shown that this energy resolution can be achieved by using production PWO crystals with APD readout. Fig. 3 shows the distributions of the stochastic and constant terms of the energy resolution measured in  $3 \times 3$  PWO crystals readout with one APD per crystal [1]. Based on this result, two APDs instead of one APD is designed for each crystal, so that the stochastic term will be reduced to 2.5% [1]. Fig. 4 shows 0.45% energy resolution reconstructed for 280-GeV electrons [1].

The overall construction of the ECAL is in progress. In the last seven years, extensive R&D has been carried out by CMS in collaboration with manufacturers to develop PWO crystals and avalanche photodiodes. Both PWO crystals and APDs are now in mass production. The barrel PWO crystals are contracted to the Bogoroditsk Techno-Chemical Plant (BTCP) in Tula, Russia, and the APDs are produced at Hamamatsu Photonics, Inc. As of this writing, about 20 000 PWO crystals out of 62 000 in the barrel have been delivered. PWO crystals are also being mass produced at Shanghai Institute of Ceramics (SIC), in Shanghai, China [2]. The delivery of all 124 000 APDs will be completed by the end of 2003. Crystals and APDs are being assembled to submodules (10 crystal), modules (40 or 50 submodules) and supermodules (1700 crystals in four modules) at two regional centers. One is in Lab27 at CERN and the other at INFN/ENEA, Rome. By the end of 2003 about 40 modules, or 10 supermodules, are completed. Fig. 5 shows two completed supermodules in Lab27 at CERN.

## III. PWO CRYSTAL RADIATION DAMAGE

Because of high energy and high luminosity of the LHC the entire CMS detector will be operated in a severe radiation environment. Fig. 6 shows the electromagnetic radiation environment expected by the CMS PWO ECAL at LHC [1].

Manuscript received November 7, 2003. This work was supported in part by the U.S. Department of Energy by Grant DE-FG03-92-ER40701.

The author is with the California Institute of Technology, Pasadena, CA 91125 USA (e-mail: zhu@hep.caltech.edu).

Digital Object Identifier 10.1109/TNS.2004.832804

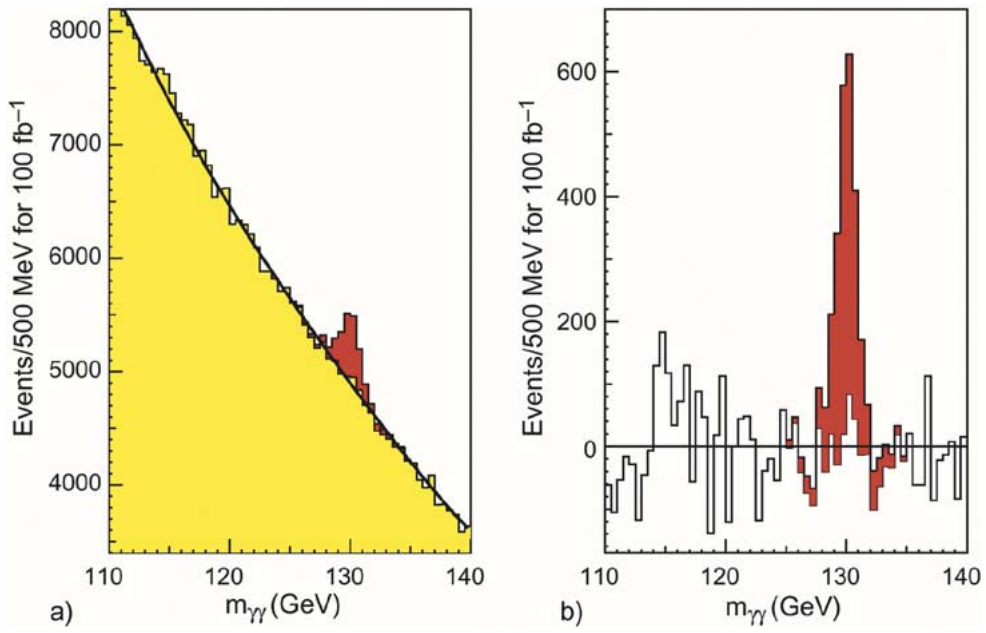


Fig. 1. A simulated 130-GeV Higgs signal, reconstructed by using an electromagnetic calorimeter with energy resolution of  $2\%/\sqrt{E} \oplus 0.5\%$ , for  $H \rightarrow \gamma\gamma$  channel with integrated luminosity of  $100 \text{ fb}^{-1}$  before (left) and after (right) background subtraction.

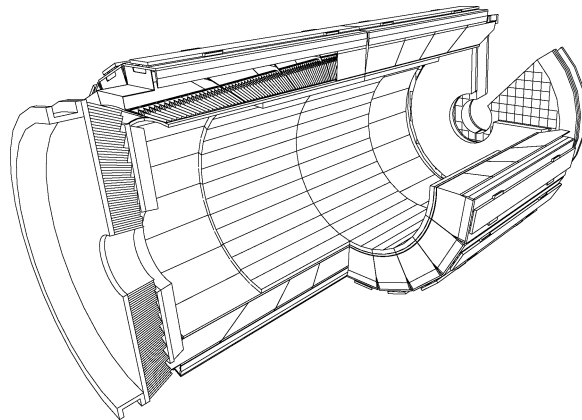


Fig. 2. A 3-D cut-away view of the CMS PWO ECAL.

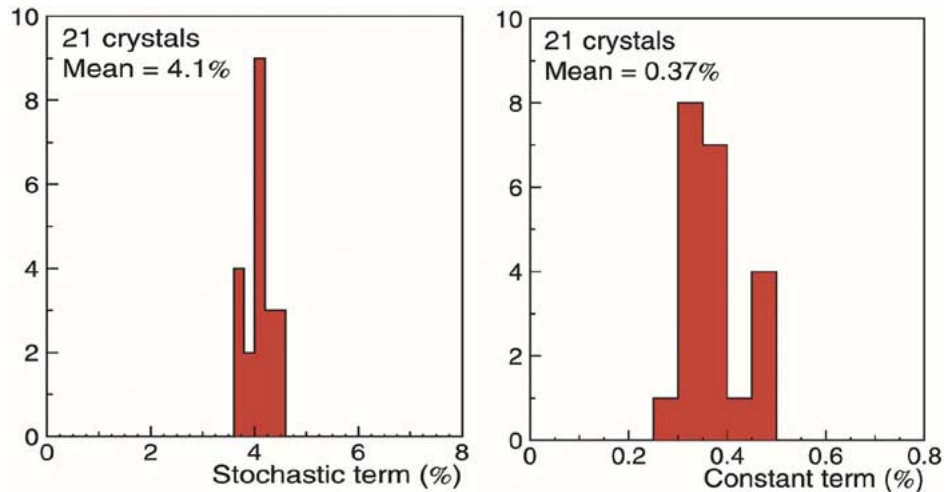


Fig. 3. The stochastic (left) and constant (right) terms of the energy resolution measured in CERN beam test.

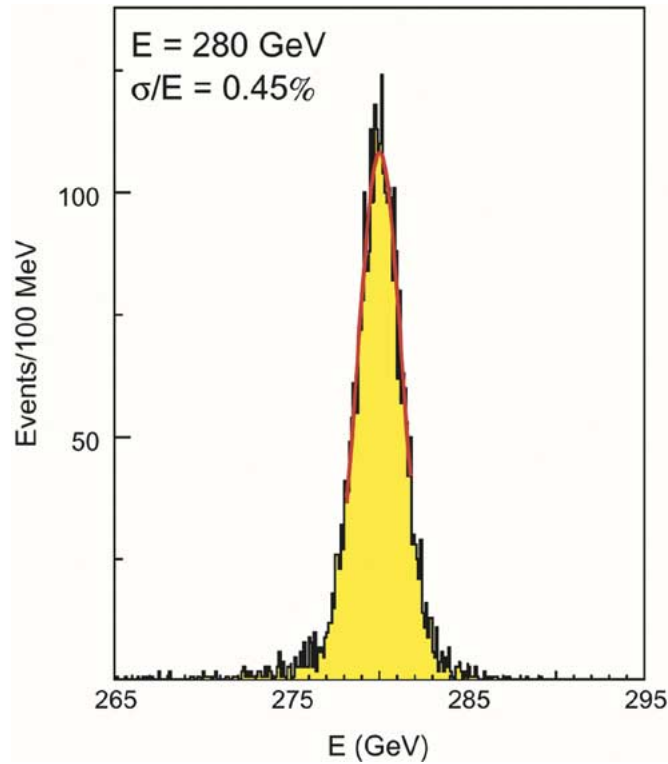


Fig. 4. Energy distribution of 280 GeV electrons measured at CERN beam test.



Fig. 5. A photo showing two supermodules in Lab27 at CERN.

The mass-produced lead tungstate crystals suffer from non-negligible radiation damage [2]. After several years of R&D, radiation damage in PWO crystals is fairly well understood. Fig. 7 shows no variation was observed in the excitation and emission spectra measured before and after  $\gamma$ -ray irradiations, indicating no damage in the scintillation mechanism. Radiation damage, however, is observed in the formation of radia-

tion induced color centers, as illustrated in the transmittance spectra shown in Fig. 8. Because of the equilibrium between color center's formation process and its annihilation process, the level of radiation damage in PWO crystals is dose rate dependent [3], as shown in Figs. 9 and 10.

It is also understood that radiation damage in PWO crystals is originated from structure defects, such as oxygen vacancies [3],

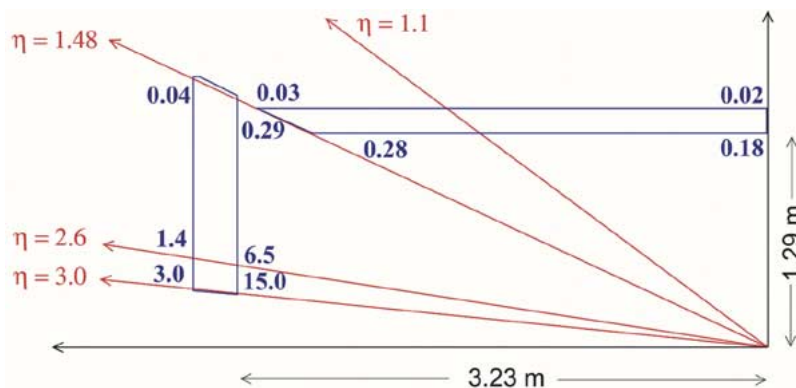


Fig. 6. Expected dose rates in Gy/h at various places of the ECAL for a luminosity of  $10^{34} \text{ cm}^{-2}\text{s}^{-1}$ . The values given at the front of the ECAL are those obtained at shower maximum.

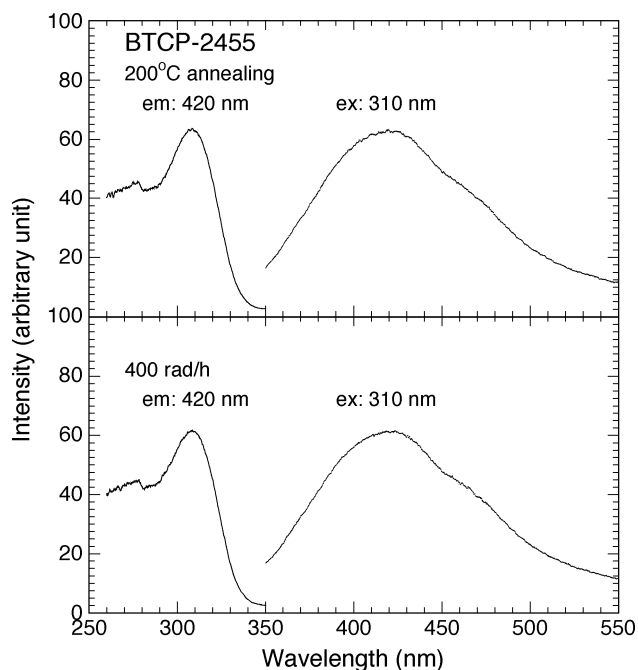


Fig. 7. The excitation and emission spectra before and after irradiation at 400 rad/h are shown as function of wavelength for sample BTCP-2455.

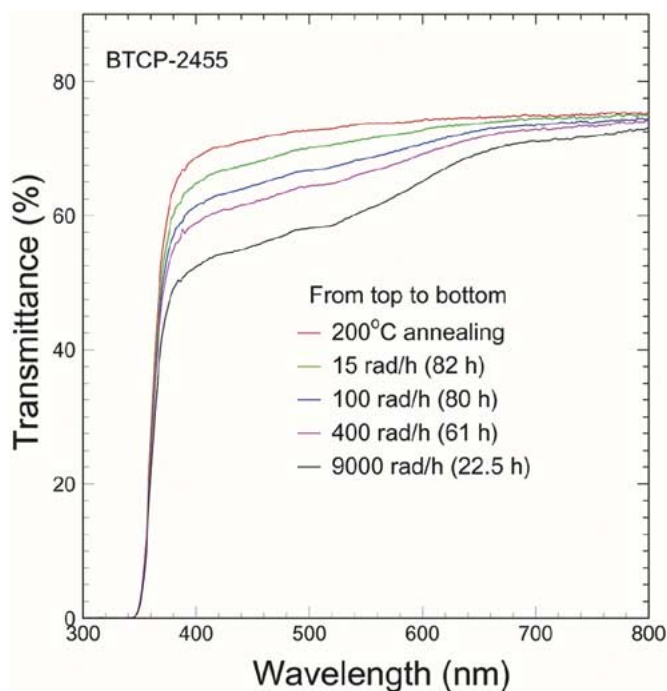


Fig. 8. The transmittance spectra at equilibrium under irradiations of several dose rates are shown as function of wavelength for sample BTCP-2455.

and there exist no correlations between PWO crystal’s radiation hardness and its initial longitudinal transmittance [2].

#### IV. MONITORING

After PWO crystals with adequate radiation hardness are produced, calibration is the key to maintain crystal precision *in situ* at LHC. Electrons from Z and W decays will be used to determine the ECAL calibration during LHC operation [1]. Other physics processes, such as electrons pairs from  $J/\psi$  and  $\Upsilon$  decays [4] as well as photon pairs from  $\eta$  decays [5], may also be used. Since PWO crystal’s scintillation mechanism is not affected by radiation, and the loss of its light output is due only to absorption caused by the radiation induced color centers, the short term variation (damage and recovery) of PWO light output

can be taken care of by using a light monitoring system which measures the variations of crystal’s transmittance and predicts the variations of its light output. To continuously measure these variations, monitoring light pulses are planned to be sent to the crystals in the  $3 \mu\text{s}$  time gaps, which are scheduled every 88.924  $\mu\text{s}$  in the LHC beam cycle [6].

The monitoring wavelength was determined by using a test bench, which measured PWO crystals’ light output and transmittance as a function of wavelength with precisions of 1% and 0.5%, respectively, [7]. Fig. 11 shows typical correlations between the relative variations of the transmittance ( $\Delta T/T$ ) and the light output ( $\Delta LY/LY$ ) for the monitoring light at four different wavelengths: (a) 410; (b) 440; (c) 490; and (d) 520 nm, for a yttrium-doped PWO sample SIC-S762. The correlation was fit to a linear function:  $(\Delta T)/(T) = \text{slope} \times (\Delta LY)/(LY)$ . The

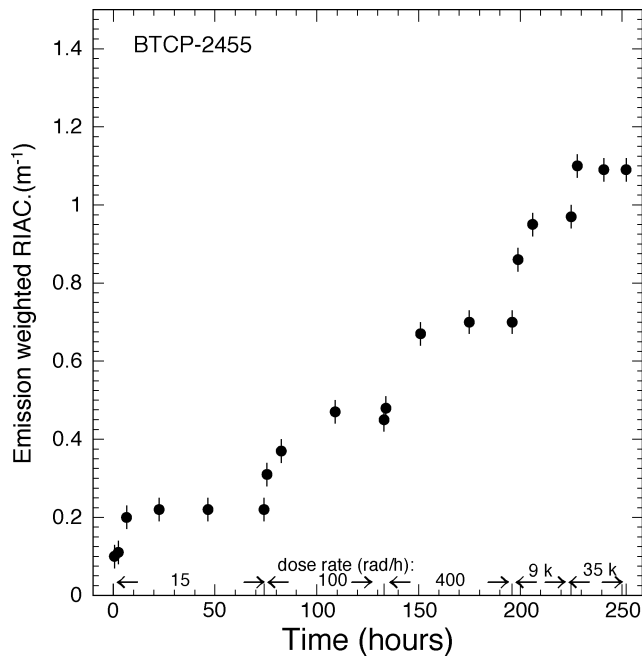


Fig. 9. The history of the emission weighted radiation induced absorption coefficient (RIAC) is shown as function of time for sample BTCP-2455.

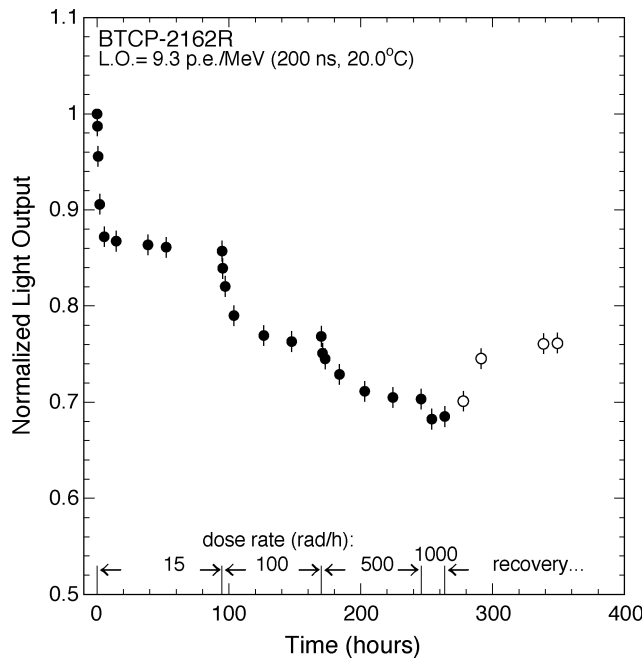


Fig. 10. The history of the light output is shown as function of time for sample BTCP-2162.

linearity ( $\chi^2/\text{DoF}$  of the fit) is generally good when light output loss is less than 10% [8].

Fig. 12 shows the monitoring sensitivity (the slope) and the linearity as a function of the monitoring wavelength for sample BTCP-2162. Also shown in the figure is the PMT quantum efficiency weighted radio luminescence. The higher monitoring sensitivity at shorter wavelength is understood because of the poorer initial transmittance as compared to that at the longer

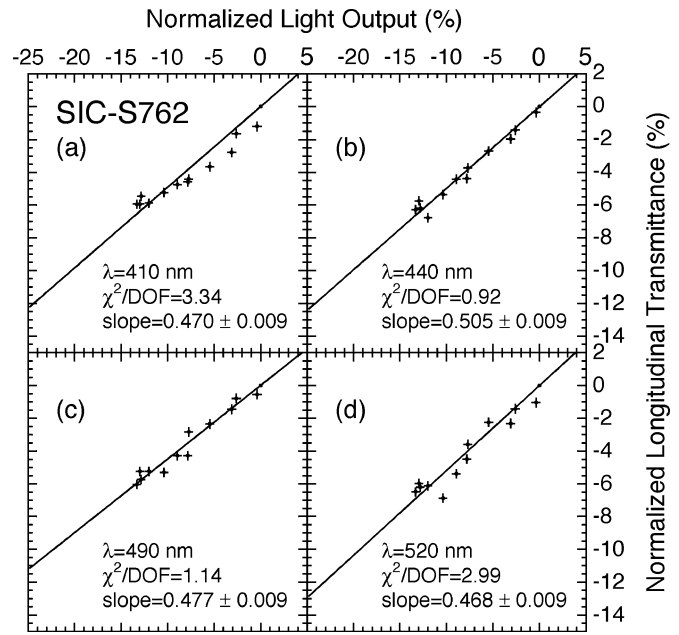


Fig. 11. Correlations between the relative variations of transmittance and light output are shown for a yttrium-doped sample SIC-S762.

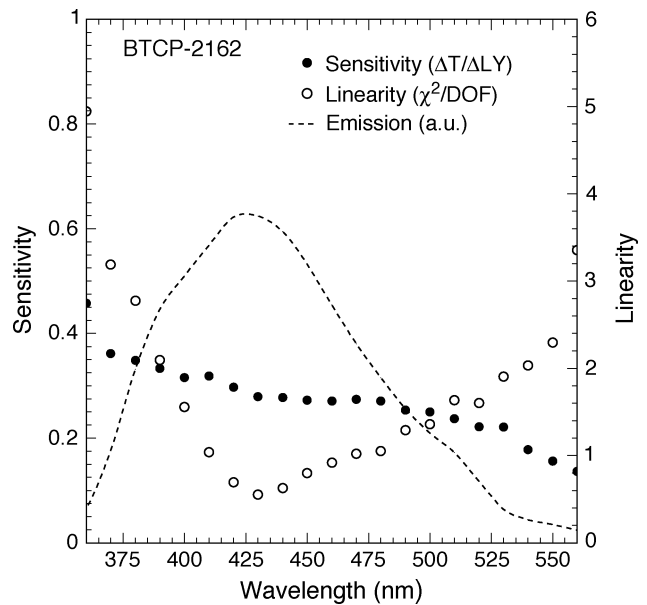


Fig. 12. Monitoring sensitivity, linearity, and emission spectrum (dashed lines) are shown for sample BTCP-2162.

wavelength. The best linearity around the peak of the radio luminescence is understood by two radiation-induced color centers peaked at the two sides of the luminescence peak with different damage and recovery speed [7]. Based upon this result, 440 nm was chosen as the monitoring wavelength with 495 nm as cross-check wavelengths. In addition, 709 and 796 nm are used to monitor independently the gain variations of the readout electronics chain from the APD to the ADC.

Fig. 13 is a schematic showing the design of the monitoring light source, which consists of three sets of lasers with corresponding diagnostics, a  $2 \times 1$  switch, a  $1 \times 80$  switch, a monitor and a controller. Each set of lasers consists of an Nd:YLF

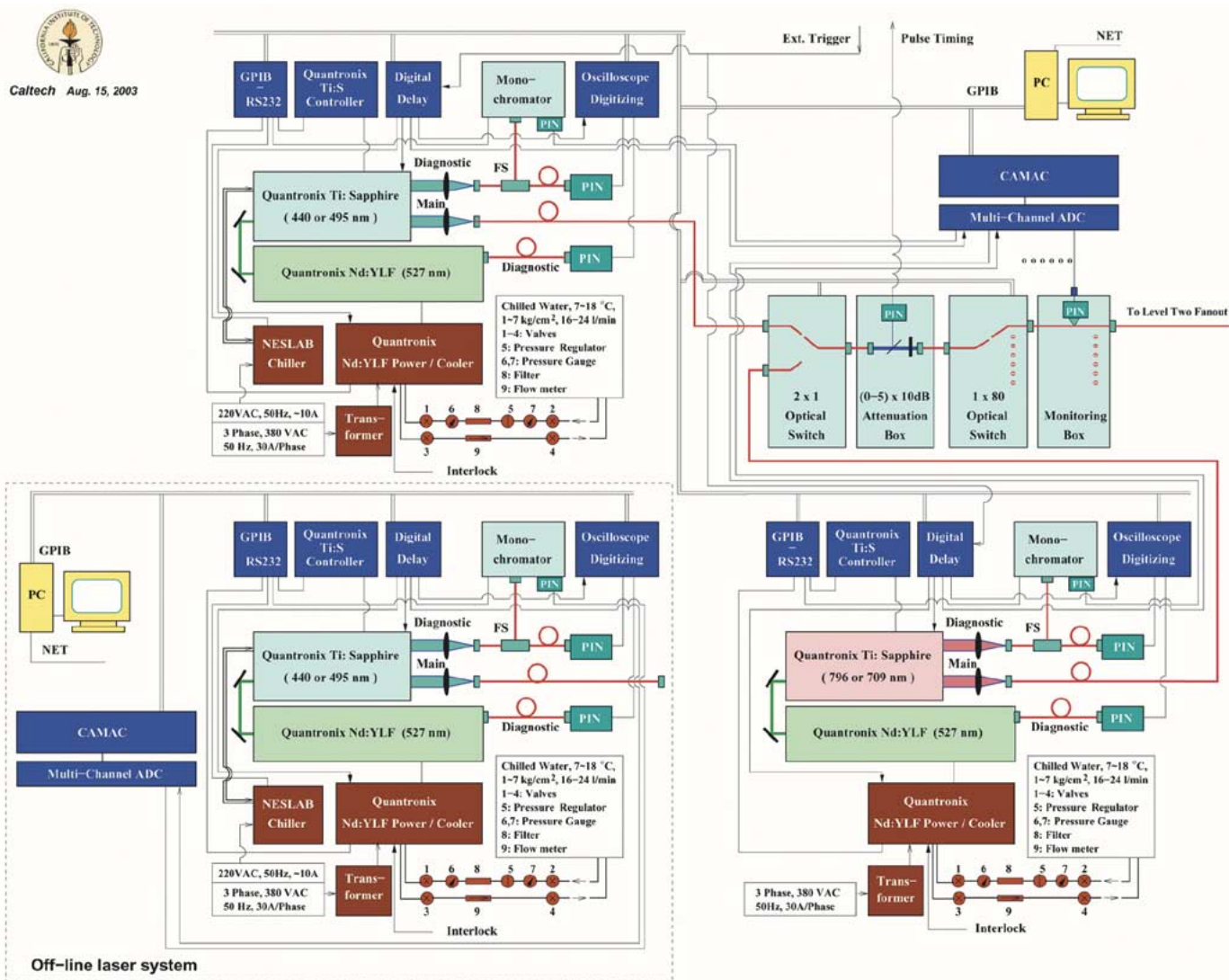


Fig. 13. A schematic showing the design of the laser based monitoring light source and high level distribution system.

pump laser and a tunable Ti:Sapphire laser with dual wavelength. Using the  $2 \times 1$  switch, up to four wavelengths (440, 495, 709, and 796 nm) are available. The spare laser system guarantees 100% availability of monitoring light source at 440 nm even during laser maintenance. Each laser set has a main and a diagnostic output. The latter is used to monitor laser pulse shape and wavelength. The parameters of the entire system are set by a PC running laser DAQ, which also collects overall information of laser performance, e.g., pulse energy, width, timing, and wavelength.

The first laser system and its corresponding diagnostics were installed and commissioned at CERN in 2001 [9], and was used in ECAL beam test since then. The other two laser systems were installed and commissioned at CERN in 2003 [10]. Fig. 14 shows consistent linearity between the electron data and the monitoring data obtained by using 440 nm laser pulses from the first laser system at CERN, where irradiation and recovery cycles simulating the LHC was applied to the crystal. It is also known that the shape of crystal's light response uniformity does not change if the degraded light attenuation length is longer than five times crystal length, and if so no degradation in calorimeter

energy resolution [3]. Fig. 15 shows the 120-GeV electron data, reconstructed with sum of nine crystals employing light monitoring corrections. The energy resolutions, measured before (run 11 094) and after (run 11 186) beam irradiations of about 650 rad, are consistent although the light output of the central crystal in the matrix was degraded by about 10% [11]. This indicates that the precision of a crystal calorimeter may indeed be maintained in a radiation environment even for crystals suffering from radiation damage.

V. SUMMARY

Over the last seven years, the CMS collaboration has taken on a challenging project to build a precision PWO crystal calorimeter for LHC. After extensive R&D high quality PWO crystals and APDs are in mass production, and detector construction is well under way. Radiation damage in PWO crystals is understood. Variations of PWO crystal's light output *in situ* are to be corrected by using the variations of crystal's transmittance measured by a laser based light monitoring system. Test beam data shows that the quality of current mass produced

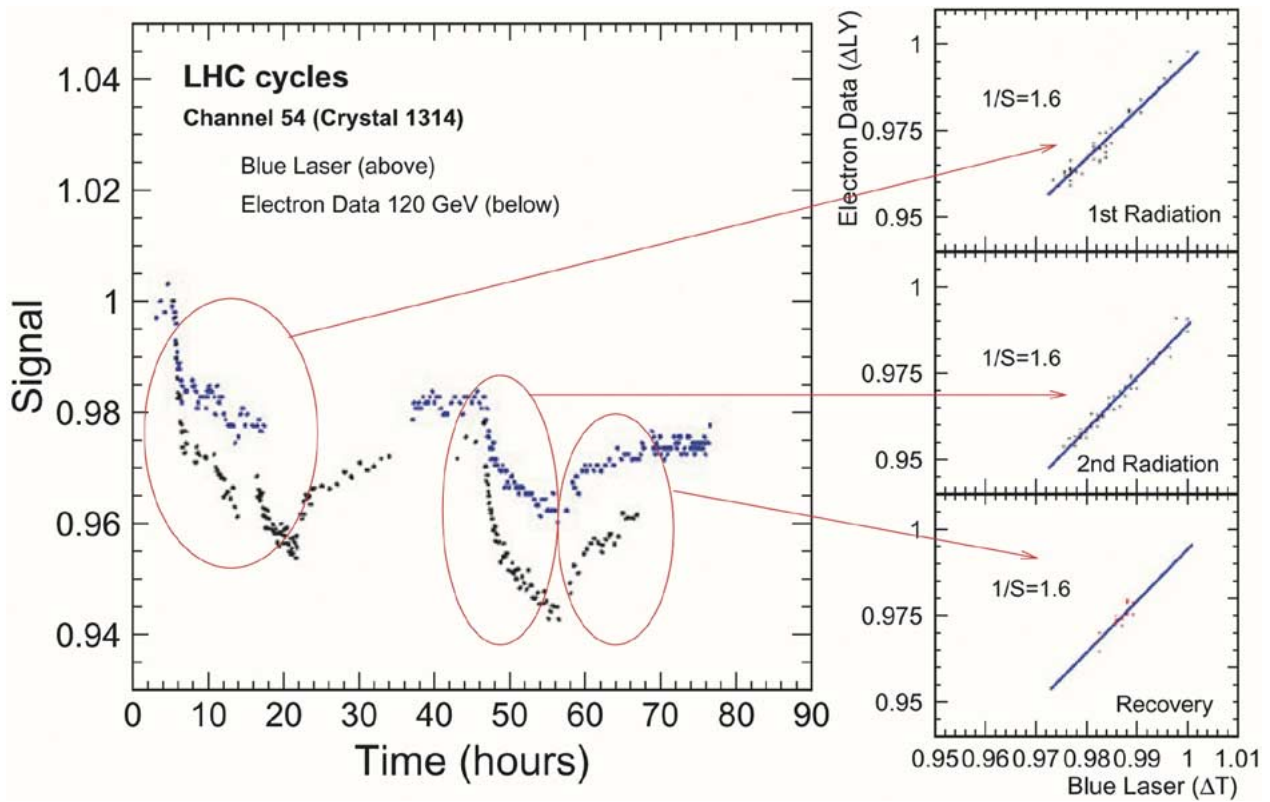


Fig. 14. History of electron (120 GeV) and laser (440 nm) data obtained during 2002 beam test are shown as function of time for PWO radiation damage and recovery. Three expansions at right show the same linearity between electron and the monitoring signals.

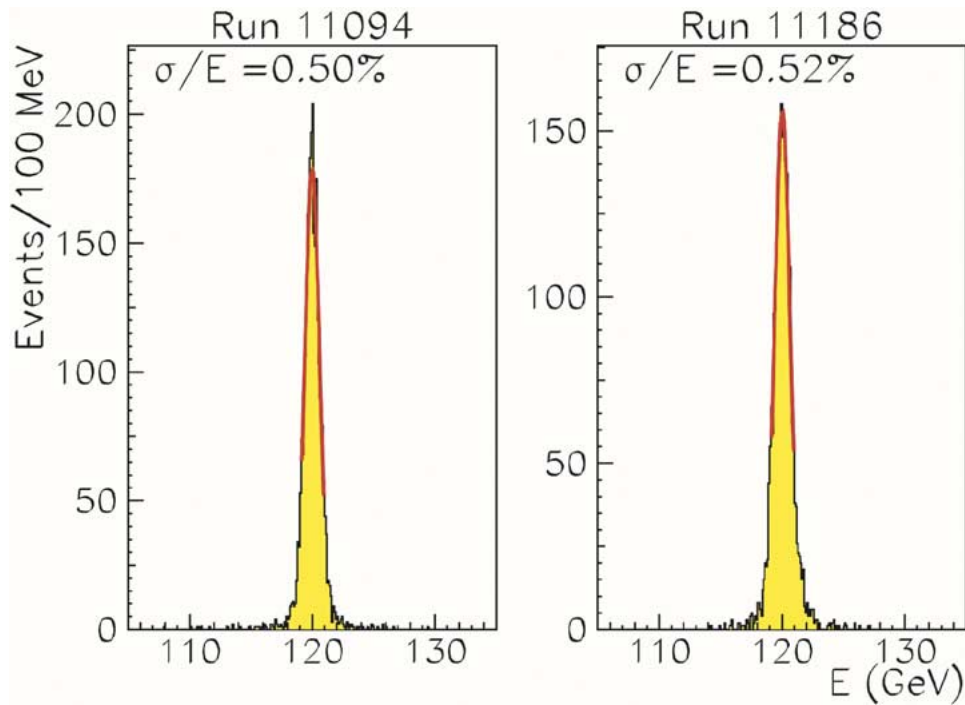


Fig. 15. 120-GeV electron energy spectra, reconstructed by summing nine crystals with light monitoring corrections, are shown before and after 650 rad irradiation.

PWO crystals is adequate to preserve the crystal precision in the severe radiation environment expected at LHC. This is an important development for precision crystal calorimetry in a radiation environment.

#### ACKNOWLEDGMENT

The author wishes to thank the CMS ECAL colleagues, especially Dr. J. Rander and P. Verrecchia, for productive collaboration.

## REFERENCES

- [1] The CMS Electromagnetic Calorimeter Project, CERN/LHCC 97-33, 1997.
- [2] R. H. Mao, L. Y. Zhang, and R. Y. Zhu, "Quality of mass produced lead tungstate crystals," in *2003 IEEE Nuclear Science Symp. Conf. Rec.*, Paper N5-6. to be published in IEEE Trans. Nucl. Sci..
- [3] R. Y. Zhu, "Radiation damage in scintillating crystals," *Nucl. Instrum. Methods*, vol. A413, pp. 297–311, 1998.
- [4] T. Hu, L. Xia, and R. Y. Zhu, "Absolute calibration of electromagnetic calorimeter at LHC with physics processes," in *Proc. 10th Int. Conf. Calorimetry in Particle Physics*, R. Y. Zhu, Ed., 2002, pp. 459–468.
- [5] C. Shevchenko. Using  $\eta \rightarrow \gamma\gamma$  process for ECAL calibration [Online]. Available: <http://cmsdoc.cern.ch/Physics/egamma/transparencies/m90-3.pdf>
- [6] "The LHC Conceptual Design Rep.," The LHC Study Group, CERN/AC/95-05, vol. 46, Oct. 1995.
- [7] X. D. Qu, L. Y. Zhang, and R. Y. Zhu, "Radiation induced color centers and light monitoring for lead tungstate crystals," *IEEE Trans. Nucl. Sci.*, vol. V47, pp. 1741–1747, 2000.
- [8] L. Y. Zhang, K. J. Zhu, R. Y. Zhu, and D. T. Liu, "Monitoring light source for CMS lead tungstate crystal calorimeter at LHC," *IEEE Trans. Nucl. Sci.*, vol. V48, pp. 372–378, 2001.
- [9] L. Y. Zhang, K. J. Zhu, R. Y. Zhu, and D. T. Liu, Installation of the ECAL monitoring light source. CMS Internal Note 2001/008.
- [10] D. Bailleux, A. Bornheim, L. Y. Zhang, K. J. Zhu, R. Y. Zhu, and D. T. Liu, ECAL monitoring light source at H4. CMS Internal Note 2003/045.
- [11] E. Auffray, P. Baillon, D. Barney, G. Bassompierre, Y. Benhammou, and A. Blik *et al.*, "Beam tests of lead tungstate crystal matrices and a silicon strip preshower detector for the CMS electromagnetic calorimeter," *Nucl. Instrum. Methods*, vol. A412, pp. 223–237, 1998.